

# ANALYTIC WAVELETS APPLIED FOR THE DETECTION OF MICROCALCIFICATIONS. A TOOL FOR DIGITAL MAMMOGRAPHY

Silvio Montrésor(1), Maria J. Lado(2), Pablo G. Tahoces(3), Miguel Souto(4), and Juan J. Vidal(4)

(1) Laboratoire d'Acoustique de l'Université du Maine Avenue Olivier Messiaen, 72085 Le Mans Cedex 9, France. phone: +33 (0)243833280 fax:+33(0)243833520, email: silvio.montrésor@univ-lemans.fr

(2) Dept. of Computer Science. University of Vigo. Campus Lagoas-Marcosende s/n. 36200 Vigo.

(3) Dept. of Electronics and Computer Science. University of Santiago. Campus Sur s/n. 15782 Santiago.

(4) Dept. of Radiology. Complejo Hospitalario Universitario de Santiago (CHUS). University of Santiago. 15782 Santiago.

## ABSTRACT

Computerized methods to detect microcalcifications in digital mammograms are being developed. Parallel to this, Wavelet Transform (WT) has become an important tool in the field of signals and images processing. This paper is devoted to the realisation and evaluation of an Analytic Wavelet Transform (AWT) based algorithm for the detection of microcalcifications. AWT has proved to be an efficient tool to detect singularities in real signals. The presented algorithm exploits the flexibility of the transform to reach any resolution at any spatial frequency. To evaluate the numerical results, Receiver Operating Characteristic (ROC) curves are calculated for several sets of parameters. Results are compared with those obtained with a previously published algorithm using a Discrete Wavelet Transform (DWT).

## 1. INTRODUCTION

Screen-film based mammography is an effective method for the early detection of breast cancer. During the last two decades, Computer-Aided Diagnosis (CAD) systems have been developed to help radiologists, in the interpretation of mammograms, but leaving the final decision to the radiologist. Digital mammography is arising as a promising technique, because each part of the breast imaging chain can be optimized. An early sign that indicates the existence of breast cancer in 30%-50% of the mammographically detected cases is the presence of clusters of microcalcifications, commonly found in the breast. Some researchers have employed WT for detecting microcalcifications in digital mammograms [9, 3, 7, 1]. The majority of the techniques employed in CAD systems aimed at the detection of microcalcifications in digital mammography, are based on the use of DWT.

Despite the fact that AWT is a well-known tool to analyze signals in the wavelet community, it has not been applied by the radiology and imaging communities to the automated detection of microcalcifications. The present study is aimed at improving the detection rate in our CAD system [3], employing an original wavelet algorithm to detect the microcalcifications. The novelty of this approach is based on the application of AWT techniques [5], instead of the more commonly used DWT. The process consisted in the computation of the Continuous Analytic Wavelet Transform (CAWT) for each image present in our database. Post-processing of the wavelet images was performed applying threshold values, based on the wavelets coefficients. Region growing techniques were also applied to identify the microcalcifications regions. Reduction of false positives was also performed

over the detected signals, and the detected microcalcifications were obtained.

## 2. WAVELET IN DIGITAL MAMMOGRAPHY

Applied to digital mammography, the most important application areas for the WT is the field of the automated detection of microcalcifications. This technique is being incorporated by an increasing number of researchers as a part of their CAD systems. Yoshida et al. [9] decomposed the digital mammograms with a WT, and reconstructed them using the wavelet coefficients obtained for different resolution levels. Strickland and Hahn [7] applied WT, and obtained a wavelet image by combination of several reconstruction levels. A reverse WT was then applied, and reconstructed images with the detected microcalcifications were produced. Wang and Karayiannis [8] employed wavelet-based subband image decomposition, and then reconstructed the mammograms from the subbands containing only high frequency values, corresponding to microcalcifications. Yu and Guan [10] used a combined method that included WT and gray level statistical features to segment the microcalcifications.

In previous works, we have developed a method based on the WT applied to the mammogram [3]. One-dimensional WT was applied over each vertical line constituting the image, to enhance the microcalcifications. A previous step in the implementation of the technique was the classification of the Region Of Interest (ROI) in fatty and dense, according to their tissue. The goal of this categorization was the application of an optimal orthogonal wavelet basis to each type of tissue. Several wavelet basis were tried, and best results were obtained with the Daubechies 4 for dense tissue, and the symlets 8 for fatty tissue. After the application of the WT, a threshold value was imposed to the reconstructed wavelet images, to obtain the possible points of microcalcifications. Next, region growing algorithms, contrast test, and clustering of the detected signals were performed. Four operations were performed over the wavelet images:

- Application of a threshold value obtained from the average coefficients of each wavelet image.
- Application of region growing (opening) techniques over the wavelet images, with the structure element constituted by the matrix:

$$\begin{bmatrix} 1 & 1 & 1 \\ 1 & 1 & 1 \\ 1 & 1 & 1 \end{bmatrix}$$

- Finding of local maximum values within each region delimited by region growing, in the wavelet image domain.

- Reduction of false positives, performed taking into consideration only the regions identified by the region growing algorithm. If the average gray level value of the corresponding original region is greatest than the average gray level value of the complete ROI, the region was considered as a true positive. Otherwise, it was considered as a false detection and rejected.

### 3. MATERIALS AND METHODS

Fifty-eight mammograms containing 37 clusters of microcalcifications, proved by biopsy, were used in this study. The cases were sequentially selected from the mammographic screening program currently undergoing, from 1992, at the Galicia Community, among women aged 50-64 years. This program is integrated in the European Network of Reference Centers for Breast Cancer Screening. The images were digitized at a resolution of 2000 horizontal x 2600 vertical pixels (87.5  $\mu$ /pixel) with 1024 gray levels, by using a KonicaKFRD-s laser scanner (Konica Corp, Tokyo, Japan).

Two experienced radiologists pointed out the position of the clusters, and an ROI of 256x256 pixels containing the microcalcifications was extracted in each case. The same radiologists marked the location of each microcalcification within each ROI, and these reference data were stored on a data file. Mean area of the clusters, as well as average gray level value, mean contrast and number of microcalcifications per cluster were calculated, to characterize the database of microcalcifications.

### 4. DETECTION ALGORITHM

To detect the microcalcifications, AWT was performed over each image. The processing technique consisted in the computation of the CAWT, employing a partition in channels and octaves, and favoring the average and high frequency domains. We have extracted the modulus of CAWT, to add all the channels present in the analysis. A correction was applied at the image edges, to avoid the distortion that wavelet transform may introduce at the borders of the signals.

We have performed the analysis independently in both horizontal and vertical direction, or either in horizontal or vertical direction. In this way, we have obtained three different modes, namely HS for the horizontal direction, VS for the vertical direction, and HV that combines the horizontal and vertical analysis. We have also employed three different operators: arithmetic and geometric average of the wavelet coefficients, and the maximum value of the coefficients in both directions, namely MOYGE, MOYAR, and MAXHV, respectively). There are other three parameters that have been taken in consideration: the first resolution level for the analysis, the number of octaves, and the number of channels per octaves. We have retained three different combinations for these parameters: 434, 244 and 234 (first resolution level, number of octaves, and number of channels per octave, respectively). In total, we had 5 sets of parameters to perform the analysis, taken by combinations of HV, HS, VS with MOYGE, MOYAR, MAXHV, and with 434, 234, 244.

Since the main goal of this work was to improve the detection rate of our CAD system, and to establish the benefits of using the novel AWT technique as an alternative to the more conventional analysis performed with the use of two-dimensional DWT, the symmlets, namely, SYMMLETS83 method; were also applied, and results obtained for both

types of wavelets were compared. Fig. 1 shows an example of the different images resulting from each step of the detection of microcalcifications, employing the named HV-MOYGE434 technique (combination of HV with MOYGE operator and with respectively 4,3,4 as first resolution level, number of octaves and number of channel per octaves). Upper left figure shows an original ROI containing the microcalcifications, upper right refers to the corresponding wavelet image, obtained with the application of AWT. Lower left corresponds to a processed image after the threshold application, and lower right shows the binary image containing the mask of the microcalcifications. Fig. 2 just differs from previous one as AWT is replaced by a DWT.

### 5. PERFORMANCE EVALUATION CRITERIA

To evaluate the different wavelet-based techniques developed to detect the microcalcifications, the position of each detected signal was compared to that of the real microcalcifications, which were previously and manually marked and stored on data files by the experienced radiologists.

Three different procedures, namely DIAG1, DIAG2 and DIAG3 were tried for the evaluation. The first technique is the result of the variation of a global threshold for all the images. The two resting techniques apply a different threshold value for each image. In the second method, the counting of detected signals was performed over the processed and thresholded image. The third method computed the number of detections from the same processed and thresholded image, but performing before a convolution using the structure element.

To evaluate the numerical results and to select the appropriate WT for the detection of the microcalcifications, the error rate curves and the ROC curves were calculated, for each analysis method and evaluation mode. The Equal Error Rate (EER) criteria define a threshold in a way that both false positive rate and false negative rate are equal. At this point, equality between specificity and sensitivity is achieved. Other important parameter that has been retained for the evaluation, is the maximum of sensitivity, namely MAXSENS, which corresponds to the minimum value of the false negatives rate. Furthermore, the MAXSENS parameter provides the maximum capability of the evaluated method to detect microcalcifications.

### 6. RESULTS AND DISCUSSION

Several sets of parameters providing different WT were used to determine the effect of the wavelet selection to detect microcalcifications, and tried over 37 ROIs of 256x256 pixels. To evaluate the performance of each wavelet transform, the corresponding ROC curves were generated using the LABROC1 program [6, 2], and the EER and MAXSENS parameters were calculated. Fig. 3 shows an example of the ROC curve obtained for the HVMOYAR method. Evaluations concerning the MAXSENS parameter has been reported on Tab. 2.

Some conclusions can be derived from the experimental results. The best absolute sensitivity is obtained for the HVMOYAR234 method, which yields a sensitivity value of 87.83% for the column corresponding to the DIAG2 method, which applies a local threshold value for each image, computing the number of detections from the processed and thresholded image. This means that a very high percentage

of the microcalcifications present in the ROIs (87.83%) have been detected with the application of the HVMOYAR234 method. For the other columns, providing the experimental results for the other developed methods, best results are obtained for HVMOYGE234 over the DIAG1 column, and for the SYMMLETS83 method, over the DIAG3 column. Results reveal differences between horizontal and vertical modes. Precisely, vertical modes are better than horizontal modes for both DIAG1 and DIAG2 methods. Tendency is inverted with the DIAG3 technique. The single modes run globally worst than the combined modes. The type of operator also affects the results. Globally, operators can be sorted from best to worst performance as follows: geometric mean, arithmetic mean and the maximum value of the coefficients in both the horizontal and the vertical modes. Related to the EER value, evaluations have been reported on Tab. 1. The best absolute value is obtained with the HVMOYAR434 method, evaluated with DIAG2. Moreover, in most cases, worst results are obtained with the SYMMLETS83 method. Similar to the MAXSENS parameter, the different methodologies are distinguishable from the data. With the exception of the SYMMLETS83 method, DIAG2 provides better results than DIAG3, being the mean EER value, in each case, 50% and 85%, respectively. The influence of the channel decomposition is also noticeable, yielding the 434 combinations best results than the other combinations tried. The type of operator employed has also importance, and best results are obtained with the MOYGE operator, independently from the channel decomposition. In the same way, the MAXHV operator yields the worst results. Comparing horizontal and vertical modes, we can perform similar observations than in the case of the MAXSENS parameter. Vertical modes perform better than the horizontal modes for the DIAG2 technique, but the tendency is inverted with the DIAG3 method, although the differences are not significant. We can deduce the following observations: the channel decomposition does not produce better results when using 4 octaves instead of 3, which means that the 4th octave band does not contain significant information concerning the microcalcifications. Moreover, the consideration of both the horizontal and the vertical modes is needed for an accurate detection, and their combination must be achieved according geometric mean operation. Finally, the comparison of the SYMMLETS83 method with other AWT methods reveals significant differences in the methodology used. Considering the DIAG2 evaluation results, the SYMMLETS83 method clearly provides the worst results: smallest maximum sensitivity and highest EER value. Taking into account DIAG3 evaluation, the SYMMLETS83 method yields a better maximum sensitivity and a high ERR value, but not the best EER value. It must be pointed out that DIAG2 is an evaluation method that benefits the accuracy of the analysis, considering the raw data, while the DIAG3 technique takes into account the complete detection scheme with post-processing. We can also compare the results obtained with the use of the best performing AWT method, the HVMOYAR234, to that obtained in our previous studies, employing DWT, where we achieved an average sensitivity of 65.94%, for the detection of microcalcifications in ROIs. With the HVMOYAR234, sensitivity increases to 87.83%, which is a remarkably higher detection rate. Moreover, with this technique, discrimination between both dense and fatty ROIs is not needed, this allowing to improve the CAD process, since the radiologist is not required

to examine the tissue of the images. In this work, we have developed several wavelet-based algorithms to detect microcalcifications in mammograms. Detection of microcalcifications can be a difficult mission for radiologists, which requires both effort and experience. Although it is important to obtain a high sensitivity, it must be considered that individual microcalcifications are not, in most cases, clinically relevant, while the clustered microcalcifications appear in an important number of cases of breast carcinoma. Although it is not necessary to detect all the microcalcifications belonging to a cluster, for the cluster to be detected, it is important to maintain a high detection rate for the individual microcalcifications, since the cluster will have a higher probability to be detected if a great number of the microcalcifications composing it are previously detected. Finally, in order to obtain a confident measure of the performance of our methods, all the techniques were applied over the same database, constituted by 37 ROIs, previously extracted from the original mammograms.

## 7. CONCLUSION

Previous works [4] have demonstrated the ability of wavelet transforms to enhance and detect microcalcifications, from an inhomogeneous background.

In this work, we have developed AWT based methods to detect microcalcifications in ROIs of digital mammograms. The results obtained were also compared to that yielded by the more commonly used DWT, and with our previous results. Best results were achieved employing the AWT based on a first resolution level that matches a level decomposition of 2, composed by 3 octaves, and with 4 channels per octave. This algorithm provided a sensitivity of 87.83% for the detection of individual microcalcifications. We can conclude that an analytic wavelet-based method can be used to help radiologists, as second readers, in the detection of microcalcifications, and subsequently, in the early diagnosis of breast cancer.

## REFERENCES

- [1] H.D. Cheng, J. Wang, and X. Shi, "Microcalcification detection using fuzzy logic and scale space approaches," *Pattern Recognition*, vol. 37, pp. 363-375, 2004.
- [2] ] M.A. Gavrielides, J.Y. Lo, and C.E. Floyd, "Parameter optimization of a computer-aided diagnosis scheme for the segmentation of microcalcification clusters in mammograms," *Med. Phys.*, vol. 29, pp.475-483, 2002.
- [3] M. J. Lado, P. G. Tahoces, A. J. Mendez, M. Souto, and J. J. Vidal, "A wavelet-based algorithm for detecting clustered microcalcifications in digital mammograms," *Med. Phys.*, vol. 26, pp. 1294-1305, 1999.
- [4] M. J. Lado, P. G. Tahoces, A. J. Mndez, M. Souto, and J. J. Vidal, "Evaluation of an automated wavelet-based system dedicated to the detection of clustered microcalcifications in digital mammograms," *Med. Inf. Internet Med.*, vol. 26, pp. 149-163, 2001.
- [5] S.G. Mallat, *A wavelet tour of signalprocessing*. San Diego: Academic Press, 1999.
- [6] C.E.Metz,"Some practical issues of experimental design and data analysis in radiological ROC studies," *Invest. Radiol.*, vol. 24, pp. 234-245, 1989.

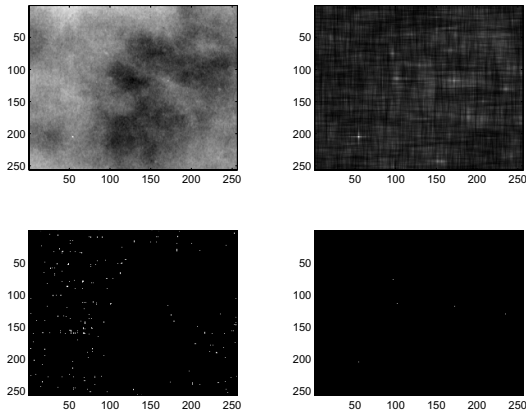


Figure 1: AWT analysis of an ROI.

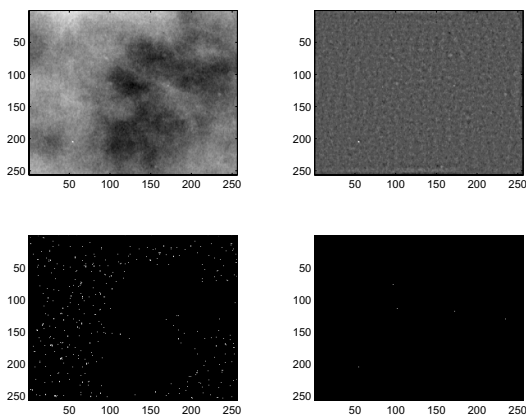


Figure 2: DWT analysis of an ROI.

- [7] R. N. Strickland, and H. II Hahn, "Wavelet transforms for detecting microcalcifications in mammograms," *IEEE Trans. Med. Imag.*, vol. 15, pp. 218-229, 1996.
- [8] T. C. Wang, and N. B. Karayiannis, "Detection of microcalcifications in digital mammograms using wavelets," *IEEE Trans. Med. Imag.*, vol. 17, pp. 498-509, 1998.
- [9] H. Yoshida, K. Doi, R. M. Nishikawa, M. L. Giger, and R. A. Schmidt, "An improved computer-assisted diagnostic scheme using wavelet transform for detecting clustered microcalcifications in digital mammograms," *Acad. Radiol.*, vol. 3, pp. 621-627, 1996.
- [10] S. Yu, and L. Guan, "A CAD system for the automatic detection of clustered microcalcifications in digitized mammogram films," *IEEE Trans. Med. Imag.*, vol. 19, pp. 115-126, 2000.

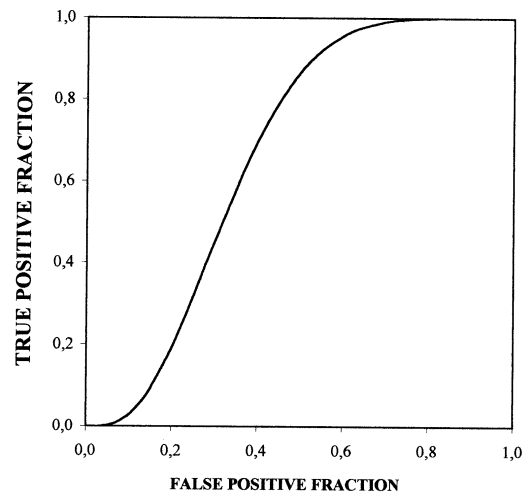


Figure 3: Example of ROC curve obtained with AWT.

MAXSENS	DIAG1	DIAG2	DIAG3
HVMOYGE434	72.75	85.34	22.54
HVMOYAR434	63.07	85.20	19.78
HVMOYGE234	<b>79.39</b>	86.86	24.20
HVMOYAR234	78.98	<b>87.83</b>	22.82
VSMOYGE234	77.59	79.53	18.67
SYMMLETS83	75.93	57.95	<b>39.83</b>

Table 1: Results obtained for the MAXSENS parameter.

EER	DIAG1	DIAG2	DIAG3
HVMOYGE434	57.58	44.40	<b>80.64</b>
HVMOYAR434	59.47	<b>36.38</b>	82.43
HVMOYGE234	57.81	58.64	81.88
HVMOYAR234	<b>51.73</b>	57.68	83.68
VSMOYGE234	60.58	58.37	85.06
SYMMLETS83	94.05	89.76	87.97

Table 2: Results obtained for the EER parameter.